Radiology: Imaging Cancer

ORIGINAL RESEARCH

Characterization and Prediction of Signal Intensity Changes in Normal Liver Parenchyma on Gadoxetic Acid–enhanced MRI Scans after Liver-directed Radiation Therapy

Anthony D. Nehlsen, MD • Kunal K. Sindhu, MD • Thomas Wolken, MS • Fahad Khan, MD • Christopher K. Kyriakakos, MD • Stephen C. Ward, MD • Erin Moshier, MS • Bachir Taouli, MD • Michael Buckstein, MD, PhD

From the Departments of Radiation Oncology (A.D.N., K.K.S., T.W., M.B.), Pathology (F.K., S.C.W.), Radiology (C.K.K., B.T.), and Biostatistics (E.M.), Icahn School of Medicine at Mount Sinai, 1184 5th Ave, 1st Floor, Box 1236, New York, NY 10029-6574. Received October 19, 2021; revision requested December 28; revision received May 17, 2022; accepted June 15. **Address correspondence to** A.D.N. (email: *Anthony.nehlsen@mountsinai.org*).

Authors declared no funding for this work.

Conflicts of interest are listed at the end of this article.

Radiology: Imaging Cancer 2022; 4(4):e210100 • https://doi.org/10.1148/rycan.210100 • Content codes: GI OI

Purpose: To better characterize and understand the significance of focal liver reaction (FLR) development in a large cohort of patients who underwent gadoxetic acid–enhanced MRI after being treated with radiation therapy (RT) for hepatobiliary tumors.

Materials and Methods: This retrospective study evaluated 100 patients (median age, 65 years [first and third quartiles, 60–69 years]; 80 men) who underwent RT for hepatocellular carcinoma, bile duct tumors, or liver metastases at Mount Sinai Hospital between March 1, 2018, and February 29, 2020. CT simulation scans were fused to MRI scans obtained 1–6 months and 6–12 months after RT, using the hepatobiliary phase of the MRI. To define FLR volume, two radiation oncologists independently delineated the borders of the hypointensity observed on MRI scans in the liver region where RT was delivered. Biologically effective dose (BED) thresholds for the formation of FLRs were calculated, along with albumin-bilirubin (ALBI) scores and grades, and overall survival.

Results: Most patients developed FLRs, which decreased in volume over time. Median BED threshold values for FLR development were 63.6 Gy at 1–6 months and 88.7 Gy at 6–12 months. While higher baseline ALBI scores were associated with a lower rate of FLRs, there was a significant association between FLR volume and increase in ALBI score at 1–6 months ($P = .048$). Twelve- and 24-month survival estimates for the cohort were 81% and 48%, respectively. Histopathologic analysis of seven explanted liver specimens demonstrated findings consistent with radiation-induced liver disease.

Conclusion: FLRs were a clear measure of liver damage after RT and were associated with the development of liver dysfunction and focal radiation-induced liver disease.

Supplemental material is available for this article.

© RSNA, 2022

Radiation therapy (RT) is an effective local treatment option for patients with cancers of the hepatobiliary system. It offers high rates of local control in the management of hepatocellular carcinoma (HCC), bile duct tumors (BTCs), and liver metastases (1–3). Normal liver parenchyma is exposed to external beam radiation as it passes through the body, potentially resulting in compromised local hepatic function. Originally described in studies of patients who underwent RT and contrast-enhanced CT follow-up imaging, focal liver reaction (FLR) represents the development of a hypointensity in an irradiated region of the liver (4–6). FLRs were found in approximately 75% of patients in these CT-based studies, with threshold doses (TDs) ranging from 13.7 Gy to 34.4 Gy delivered via various fractionation regimens. These studies also demonstrated varying patterns of FLR evolution, with peak FLR volumes occurring between 1.8 and 6 months and significant resolution seen 2 to 9 months later (4,5).

Similar studies have been conducted in patients who underwent gadoxetic acid (gadolinium ethoxybenzyl diethylenetriamine pentaacetic acid)–enhanced MRI. MRI is a dynamic, advanced form of imaging that offers important advantages in visualizing biologic changes in the liver, such as FLRs. While it is not entirely clear why FLRs occur in the manner in which they do at MRI, there is some evidence to suggest that hepatocyte injury and the associated changes in organic anion transporting peptides, which may facilitate the transport of gadoxetic acid into liver parenchymal cells, play a central role (7,8). Studies in which gadoxetic acid is used report estimated TDs for FLRs of between 28 Gy and 34.4 Gy (9,10).

Several questions remain regarding the development and evolution of FLRs at gadoxetic acid–enhanced MRI. Unlike the CT-based studies, previous MRI-based studies did not follow the progression of FLRs over time. Thus, the patterns of FLR evolution at MRI are largely unknown. Additionally, while these studies provided corresponding

This copy is for personal use only. To order printed copies, contact reprints@rsna.org

Abbreviations

ALBI = albumin-bilirubin, BTC = bile duct tumor, BED = biologically effective dose, FLR = focal liver reaction, HCC = hepatocellular carcinoma, IDL = isodose line, LBR = log binomial regression, LPR = log Poisson regression, OS = overall survival, RT = radiation therapy, RILD = radiation-induced liver disease, RR = relative risk, TD = threshold dose

Summary

Focal liver reactions (FLRs) are hypointensities in regions of irradiated liver on gadoxetic acid–enhanced MRI scans, and in this study, FLR volume was associated with and predictive of the development of liver dysfunction and radiation-induced liver disease.

Key Points

- Focal liver reactions (FLRs) were present on 72% of evaluable liver MR images obtained 1–6 months after radiation therapy (RT) and 65% of MR images obtained 6–12 months after RT.
- The findings were reproducible, with excellent interrater agreement between physicians evaluating the MR images at both the 1–6-month ($\kappa = 0.82$) and 6–12-month ($\kappa = 0.83$) time points.
- While higher baseline albumin-bilirubin (ALBI) scores were associated with lower prevalence of FLRs, there was a significant association between FLR volume and increase in ALBI score at 1–6 months ($P = .048$).

Keywords

MRI, Radiation Therapy

isodose lines (IDLs), it is unclear which biologically effective dose (BED) is associated with the development of FLRs. This is particularly important when assessing FLRs across the wide range of dose fractionation regimens currently being used in clinical practice (11). Furthermore, the dosimetric and clinical factors that predict development of FLRs, and the reasons that some patients do not demonstrate this finding at follow-up imaging, are unknown. Finally, the relationship between FLR development and short- and long-term toxicity remains unclear. Histologic analysis of FLRs has been carried out on only a small number of patients in CT-based series and no such analysis has been done in MRI-based series (12). While prior studies have evaluated the relationship between FLRs and Child-Pugh scores and/or liver enzyme tests, the data are somewhat subjective and have not always been clinically correlated. In contrast, albumin-bilirubin (ALBI) scores may be more predictive of survival outcomes and the development of toxicity in many of these patients (13,14). ALBI grades can be used to stratify ALBI scores as follows: less than or equal to −2.60 (ALBI grade 1), more than −2.60 to less than or equal to −1.39 (ALBI grade 2), and more than −1.39 (ALBI grade 3). Gadoxetic acid may offer a crucial advantage in visualizing liver changes after RT when compared with standard gadolinium-based imaging (15).

In this study, we examined the dosimetry and predictors of FLRs in a large cohort of patients who underwent gadoxetic acid–enhanced MRI after being treated with partial liver RT for HCC, BTCs, or liver metastases using a variety of dose fractionation regimens. We also analyzed survival data and used ALBI scores to assess for treatment-related toxicities in patients with and without FLRs. Finally, we performed histologic examination of irradiated regions of liver parenchyma in patients who underwent liver transplantation to correlate our radiologic findings to the underlying pathologic condition.

Materials and Methods

Patient Eligibility

We retrospectively identified the records of 122 consecutive patients who underwent RT to the liver for HCC, BTCs, or liver metastases at our institution between March 1, 2018, and February 29, 2020. Patients were included in this study if they were at least 18 years of age at the time they underwent RT and if they underwent follow-up imaging with gadoxetic acid–enhanced MRI 1–6 months and/or 6–12 months after completing RT. This Health Insurance Portability and Accountability Act–compliant study was approved by the institutional review board at our institution, with waiver of informed consent.

RT Techniques

All patients were treated with 6-MV photons using conventionally fractionated intensity-modulated RT ($n = 22$) or stereotactic body RT ($n = 100$). Daily imaging with cone-beam CT was used for each patient. Treatment planning and dose calculations were performed using Eclipse software (version 15.6; Varian Medical Systems) with Monte Carlo calculations.

Defining the FLR

CT simulation scans were manually fused to posttreatment MRI scans obtained 1–6 months and/or 6–12 months after RT using the hepatobiliary phase of the MRI (20 minutes after delivery of gadoxetic acid). The liver region where RT was delivered was used as the primary focus of fusion. Two radiation oncologists (a 4th-year radiology resident [A.D.N.], and a radiation oncologist with 9 years of experience treating hepatobiliary malignancies [M.B.]) independently delineated the borders of the hypointensity observed on MRI scans in the area of the liver where RT was delivered during the study period using Eclipse contouring software (10). Each rater was blinded to the other rater's measurements. The volume of the structure created as a result of this process was defined as the FLR volume.

The dose-volume histogram of the liver was obtained from the planning CT scan and used to identify the TD associated with FLR volume. This TD was then converted into a volumetric structure using the CT planning software (Eclipse). Areas that extended outside of the liver contour on the planning CT were removed. The fused MRI and planning CT were then reviewed for overlap of the TD and FLR structures as previously described by Sanuki et al (9). An example of the FLR delineation process and corresponding IDL identification is shown in Figure 1. The BED was then calculated using an α/β ratio of 8 for normal liver parenchyma (16).

Each case with no evidence of an FLR on the MRI scan obtained 1–6 months after RT was reviewed by an independent radiologist (C.K.K., 5 years of experience) to assess for hepatic parenchymal hepatobiliary phase contrast material excretion and was classified as either adequate or poor.

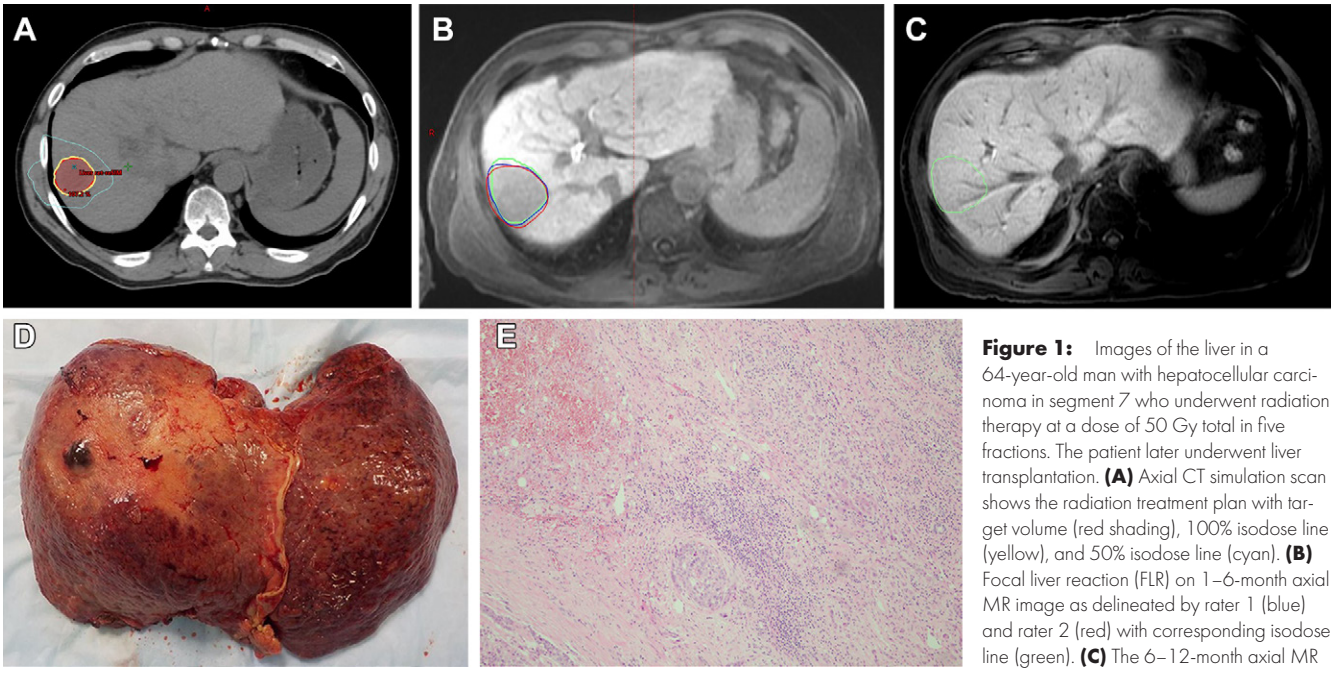


Figure 1: Images of the liver in a 64-year-old man with hepatocellular carcinoma in segment 7 who underwent radiation therapy at a dose of 50 Gy total in five fractions. The patient later underwent liver transplantation. **(A)** Axial CT simulation scan shows the radiation treatment plan with target volume (red shading), 100% isodose line (yellow), and 50% isodose line (cyan). **(B)** Focal liver reaction (FLR) on 1–6-month axial MR image as delineated by rater 1 (blue) and rater 2 (red) with corresponding isodose line (green). **(C)** The 6–12-month axial MR image shows resolution of FLR. **(D)** Gross specimen shows a circumscribed, thick plaquelike patch covering 7.0 cm (segment 7/8) of the explant surface. **(E)** Hematoxylin-eosin stain (original magnification, ×20) represents tumor regression with sinusoidal congestion, perilesional chronic inflammation, and dense fibrosis.

Patient Follow-up and Assessment of Liver Function

Patient follow-up was tracked using the electronic medical record. All patients were seen weekly during RT and scheduled for routine follow-up at 1 month after RT and every 3 months thereafter. MRI scans were identified at 1–6 and 6–12 months. If more than one MRI was available for a range of dates, the MRI conducted furthest from radiation delivery was selected. The last available date of follow-up or death was used to determine overall survival (OS). Albumin and bilirubin laboratory results were collected within 1 month prior to RT and within 1 month of both the 1–6-month and 6–12-month MRI scans. The values selected included those closest to the RT start date and the values drawn closest to 6 months (for the 1–6-month time point) and 12 months (for the 6–12-month time point). ALBI scores were calculated using the following equation: $(\log_{10}\text{bilirubin} \times 0.66) + (\text{albumin} \times -0.085)$ (17).

Pathologic Review

Formalin-fixed, paraffin-embedded tissue slices from explanted liver specimens were reassessed for treatment-related changes and residual or new malignancy by two dedicated liver pathologists (F.K., 4 years of experience; S.C.W., 18 years of experience). Treatment-related histopathologic patterns were graded following the methods previously described by Maturen et al (18).

Statistical Analysis

Patient demographic, disease-related, and treatment-related characteristics were summarized for continuous variables as median and first and third quartiles, Q1–Q3, for categorical variables as counts and percentages. Distributions of dosimetric parameters were compared between patients with and without FLRs at 1–6 months and 6–12 months using a Wilcoxon rank sum test. Interrater agreement for the presence of liver changes evident on 1–6-month and 6–12-month MRI scans was evaluated using the Cohen κ statistic. The Landis and Koch guidelines were adopted as benchmark scales of κ coefficients (moderate, 0.41–0.60; substantial, 0.61–0.80; almost perfect, 0.81–1.0). Interrater agreement for continuous variables on 1–6-month and 6–12-month MRI scans was evaluated by the intraclass correlation coefficient using a two-way random effects (patient, rater), single measure, and absolute agreement approach (19). An intraclass correlation coefficient greater than 0.90 was considered excellent agreement (20).

A multivariable generalized estimating equations model with a Poisson distribution, logarithmic link function, and an exchangeable correlation structure, to account for multiple evaluations of FLRs by two different readers, was used to estimate adjusted relative risks (RRs) and 95% CIs to identify predictors of FLRs. A log Poisson regression (LPR) with a Poisson distribution was used rather than the preferred log binomial regression (LBR) with a binomial error distribution owing to lack of model convergence. Because LBR models often have convergence issues, a modified Poisson regression model introduced by Zou (21), which combines an LPR with robust variance estimation, has been shown to be a useful alternative to LBR for estimating RRs (22). The modified Poisson regression model specifically involves fitting a generalized linear model with a Poisson distribution and logarithmic link function, and using a sandwich estimator to obtain variance estimates that are robust to the error misspecification. Carter et al (23) showed that the coefficient estimates from an LPR model consistently estimate the coefficients from an LBR model, and that the information sandwich estimator of the covariance matrix of the LPR model is a consistent estimator of the covariance matrix of estimated coefficients from an LBR model. In the context of clustered or repeated measures data, the modified Poisson regression model can be applied

within a generalized estimating equations framework with an exchangeable correction structure to account for the clustering (23). This method has been shown to perform well across a range of settings, including interventional and observational study designs with small and large numbers of clusters (24). We chose to estimate RRs instead of odds ratios via logistic regression because the latter tends to overestimate the strength of the association when the incidence of the FLRs is more than 10%, as it is in this study (25).

OS was analyzed using the Kaplan-Meier method, and those with and without FLRs were compared using the log-rank test. A Cox proportional hazards model was used to test for associations between FLR volume at 1–6 months and 6–12 months and OS. Patients with no evaluable MRI scan at the 1–6-month or 6–12-month time points were not included in the statistical analyses for the corresponding time point. All statistical analyses were performed using SAS statistical software (version 9.4; SAS Institute). *P* less than .05 was considered to indicate a significant difference.

Results

Patients

A total of 100 patients met our inclusion criteria and were analyzed in this study. Twenty-two patients did not have evaluable follow-up MRI scans and were excluded. Baseline patient characteristics are depicted in Table 1. Eighty percent of these patients were men, and the median age was 65 years (range, 37–87 years; first and third quartiles, Q1–Q3, 60–69 years). The median dose delivered was 4500 cGy in five fractions (range, 3000–6750 cGy in three to 25 fractions; first and third quartiles, Q1–Q3, 4000–5000 cGy in five fractions) using photons. Eighty-seven percent of patients were treated with stereotactic body RT, and 17% were treated with conventionally fractionated intensity-modulated RT. HCC was the most common treated malignancy (79%), followed by BTCs (13%) and metastatic lesions (8%). Twenty-nine percent of patients had a history of alcohol abuse, and 66% of patients had a history of cirrhosis, the most common causes of which were hepatitis C (37%), hepatitis B (13%), and nonalcoholic steatohepatitis (12%). Thirteen percent of patients had a history of prior RT (3% at the evaluated site in the liver and 10% at other sites), 39% had a history of prior yttrium 90 (^{90}Y) treatment, and 23% had a history of transarterial chemoembolization. Forty-seven percent of patients received systemic therapy within 1 month of (before or after) RT.

Dosimetric Parameters

FLRs and corresponding dosimetric parameters for patients with and without FLRs at 1–6 months

Table 1: Patient Characteristics

Characteristic	Value
No. of patients	100
Age (y)*	64 [60–69]
Sex	
Men	80 (80)
Women	20 (20)
ECOG	
0	73 (73)
1	21 (21)
2	5 (5)
3	1 (1)
Race	
White	36 (36)
Black	13 (13)
Hispanic	1 (1)
Asian	1 (1)
Not listed	49 (49)
Primary site	
HCC	79 (79)
Biliary tract	13 (13)
Metastasis	8 (8)
History of alcohol abuse	
No	71 (71)
Yes	29 (29)
Hepatitis type	
None	34 (34)
HepB	13 (13)
HepB and HepC	1 (1)
HepC	37 (37)
HepC and NASH	2 (2)
NASH	12 (12)
Autoimmune	1 (1)
Prior treatment	
RT+TACE+^{90}Y	1 (1)
RT+TACE	2 (2)
RT+^{90}Y	3 (3)
RT only	7 (7)
TACE+^{90}Y	7 (7)
TACE only	13 (13)
^{90}Y only	28 (28)
None	39 (39)
ALBI score*	−2.17 [−2.61 to −1.62]
Baseline ALBI grade	
1	26 (26)
2	56 (56)
3	17 (17)
Unknown	1 (1)
Systemic therapy within 1 month	
No	53 (53)
Yes	47 (47)
Dose received (cGy)*	4500 [4000–5000]
No. of fractions*	5 [5–5]
Dose/fraction*	900 [750–1000]

Note.—Unless otherwise indicated, data are numbers of patients, with percentages in parentheses. ALBI = albumin-bilirubin, ECOG = Eastern Cooperative Oncology Group, Hep = hepatitis, HCC = hepatocellular carcinoma, NASH = nonalcoholic steatohepatitis, RT = radiation therapy, TACE = transarterial chemoembolization, ^{90}Y = yttrium 90.
* Data are medians, with first and third quartiles, Q1–Q3, in brackets.

Table 2: Dosimetric Measures for Both Raters at 1–6-Month MRI Scans

Parameter	No FLR	FLR	*P* Value
Dosimetric measures for rater 1 (*n* = 94)			
No. of patients (%)	26 (28)	68 (72)	
Dose received (cGy)	4500 [4000–5000]	4800 [4000–5000]	.30
No. of fractions	5 [5–5]	5 [5–5]	.66
Dose/fraction	800 [800–900]	900 [750–1000]	.34
Liver-GTV	1419.93 [1084.38–1841.30]	1340.99 [1038.16–1635.72]	.38
PTV volume (cm^3)	65.84 [28.28–182.80]	58.48 [35.58–200.68]	.94
FLR volume (cm^3)	NA	99.10 [39.55–203.20]	NA
Dosimetric measures for rater 2 (*n* = 89)			
No. of patients (%)	24 (27)	65 (73)	
Dose received (cGy)	4500 [4000–4900]	4800 [4500–5000]	.15
No. of fractions	5 [5–5]	4 [5–5]	.63
Dose/fraction	800 [700–900]	900 [800–1000]	.21
Liver-GTV	1366.74 [931.92–1730.90]	1372.20 [1082.04–1656.00]	.71
PTV volume (cm^3)	59.15 [28.76–136.27]	76.25 [30.79–206.30]	.52
FLR volume (cm^3)	NA	101.60 [44.60–193.00]	NA

Note.—Unless otherwise indicated, data are medians with first and third quartiles, Q1–Q3, in brackets. FLR = focal liver reaction, GTV = gross target volume, NA = not applicable, PTV = planning target volume.

Table 3: Dosimetric Measures for Both Raters at 6–12-Month MRI Scans

Parameter	No FLR	FLR	*P* Value
Dosimetric measures for rater 1 (*n* = 52)			
No. of patients (%)	18 (35)	34 (65)	
Dose received (cGy)	4650 [4000–5000]	5000 [4500–5000]	.052
No. of fractions	5 [5–5]	5 [5–5]	.70
Dose/fraction	800 [800–1000]	950 [800–1000]	.52
Liver-GTV	1366.74 [1014.54–1594]	1323.87 [1135.18–1593.76]	.90
PTV volume (cm^3)	79.38 [29.23–206.30]	56.99 [22.85–138.93]	.41
FLR volume (cm^3)	NA	43.00 [15.50–110.60]	NA
Dosimetric measures for rater 2 (*n* = 48)			
No. of patients (%)	15 (31)	33 (69)	
Dose received (cGy)	4500 [4000–5000]	5000 [4500–5000]	.056
No. of fractions	5 [5–5]	5 [5–5]	.86
Dose/fraction	800 [800–1000]	1000 [900–1000]	.38
Liver-GTV	1289.74 [978.11–1594.00]	1343.45 [1159.47–1615.44]	.71
PTV volume (cm^3)	66.45 [28.28–206.30]	59.88 [25.33–138.93]	.89
FLR volume (cm^3)	NA	43.90 [25.90–99.20]	NA

Note.—Unless otherwise indicated, data are medians with first and third quartiles, Q1–Q3, in brackets. FLR = focal liver reaction, GTV = gross tumor volume, NA = not applicable, PTV = planning target volume.

and 6–12 months are depicted in Tables 2 and 3, respectively. Ninety-four MRI scans were evaluable at the 1–6-month time point, at which time 68 patients (72%) demonstrated FLRs with a median volume of 99 cm^3 (range, 10.10–649.10 cm^3; first and third quartiles, Q1–Q3, 39.55–203.20 cm^3). Of the 26 patients without an FLR at 1–6 months, 14 (54%) were determined to have poor gadoxetic acid excretion. Fifty-two MRI scans were available for analysis 6–12 months after completion of RT, at which time 34 patients (65%) demonstrated FLRs with a median volume of 43 cm^3 (range, 5.4–227 cm^3; first and third quartiles, Q1–Q3, 15.5–110.60 cm^3). The median TD for FLRs was 35.4 Gy at 1–6 months and 45.2 Gy at 6–12 months. Excellent agreement between raters was observed for the presence of liver changes on the 1–6-month (κ = 0.82;

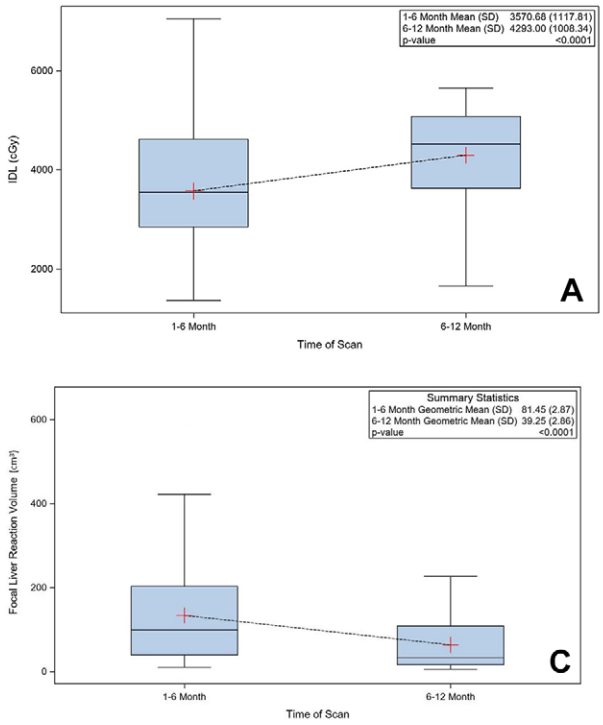


Figure 2: Dose and volume distributions corresponding to presence of focal liver reactions (FLRs) for **(A)** isodose line (IDL), **(B)** biologically effective dose (BED) IDL, and **(C)** FLR volume.

95% CI: 0.70, 0.93) and the 6–12-month (κ = 0.83; 95% CI: 0.69, 0.98) MRI scans.

Forty-five patients were evaluable at both time points. Of the 33 patients with FLRs at 1–6 months, five (15%) demonstrated complete resolution of their changes on their 6–12-month MRI scan. None of the 12 patients with no FLRs observed at 1–6 months demonstrated an FLR at 6–12 months.

Figure 2 depicts the distributions of the IDLs, BED values, and FLR volumes observed at 1–6 months and 6–12 months in patients with an observed FLR. The median FLR volume was significantly reduced at 6–12 months compared with 1–6 months (33.3 cm^3 vs 91 cm^3; $P < .001$). Additionally, the median IDL corresponding with an FLR at 6–12 months was significantly higher than that observed at 1–6 months (4519 cGy vs 3541 cGy; $P < .0001$). Finally, the median BED value corresponding to an FLR at 6–12 months was also higher than that observed at 1–6 months (8871 cGy vs 6355 cGy; $P < .0001$). Intraclass correlation coefficients were excellent at both the 1–6-month and 6–12-month time points for FLR volumes (0.94 [95% CI: 0.92, 0.96] and 0.89 [95% CI: 0.84, 0.92], respectively), IDLs (0.87 [95% CI: 0.83, 0.91] and 0.95 [95% CI: 0.92, 0.96], respectively), and BED values (0.83 [95% CI: 0.78, 0.88] and 0.92 [95% CI: 0.89, 0.94], respectively).

Predictors of FLR

The results of a multivariable analysis to identify predictors of FLRs at 1–6 months are shown in Table 4. A baseline ALBI grade of 2 (RR: 0.77; 95% CI: 0.60, 0.99; $P = .04$) or 3 (RR: 0.61; 95% CI: 0.40, 0.91; $P = .01$) was associated with a lower risk of FLRs at 1–6 months compared with a baseline ALBI grade of 1. Receipt of systemic therapy within 1 month of RT (RR: 0.74; 95% CI: 0.57, 0.97; $P = .03$) was associated with a decreased risk of FLRs. No significant increased risk of FLRs (RR: 1.35; 95% CI: 1.00, 1.82; $P = .053$) was observed for patients with a history of hepatitis B or C. Alcohol abuse, prior treatment with ^{90}Y, a history of prior RT, and the BED received from prior RT were not associated with risk of FLRs.

Assessment of Liver Function

Associations between FLR volume and liver decompensation at 1–6 months and 6–12 months, as shown by the ALBI score, are depicted in Figure 3. At 1–6 months, there was an association between FLR volume and ALBI score; for each 100 cm^3 increase in FLR volume, the ALBI score increased by 0.12 units ($P = .048$) (Fig 3A). However, when excluding the four outlier patients with FLR volumes larger than 400 cm^3, this difference was no longer appreciated. This difference was no longer evident at 6–12 months ($P = .37$) (Fig 3B). Patients with FLRs at 1–6 months (mean, 0.11 units ± 0.07 [SD]) experienced smaller increases in ALBI score than those without FLRs (mean, 0.51 units ± 0.11; $P = .002$), a difference that was not observed at 6–12 months ($P = .45$). Finally, as the ratio of FLR volume to normal liver volume (calculated as liver volume minus gross tumor volume) increased, ALBI scores at the 1–6-month time point increased ($P = .02$). However, no evidence of a difference was observed at the 6–12-month time point ($P = .53$).

Survival Estimates

OS Kaplan-Meier estimates for all patients, for those with and without FLRs at 1–6 months, and for those with and without FLRs at 6–12 months, are shown in Figure E7 (supplement). Twelve- and 24-month survival estimates for the entire cohort were 81% and 48%, respectively. No evidence of a difference in OS outcomes was observed at 12 months (85% vs 70%) or 24 months (50% vs 56%) for those with and without an FLR at 1–6 months ($P = .11$) or at 12 months (96% vs 100%) or 24 months (57% vs 70%) for patients with and without an FLR at 6–12 months ($P = .82$). There was no association between FLR volume at 1–6 months and OS (hazard ratio, 1.01; 95% CI: 0.97, 1.06; $P = .50$), which remained true at the 6–12-month time point (hazard ratio, 0.74; 95% CI: 0.53, 1.03; $P = .08$).

Histopathologic Correlation

Pathologic assessment of liver specimens from seven patients with FLR was done (Table E1 [supplement]). The median time to liver transplantation after completing RT was 10 months (range, 4–27 months). FLR was noted in all seven patients at the 1–6-month time point, with resolution of FLR at the 6–12-month time point in one patient (case 7). The findings in all seven patients were consistent with radiation-induced liver disease (RILD). An example of FLR correspondence over time with explant is shown in Figure 1. Similar examples of the other six patients are depicted in Figures E1-E6 (supplement). Three primary patterns of parenchymal response were noted at histologic analysis. An area of bandlike chronic inflammation with fibrotic tissue remodeling and hepatic parenchymal collapse was observed in six patients (three extensive, one moderate, two mild). Remodeled vascularization, endothelial injury, and sinusoidal collapse consistent with sinusoidal obstruction syndrome were evident in all seven patients (one extensive, one moderate, five mild). Frank necrosis with loss of stromal and parenchymal architecture was observed in five patients (three extensive, one moderate, one mild).

Discussion

Well-demarcated radiologic changes to normal liver tissue after RT were originally reported in multiple CT-based series (4–6). However, CT-based liver imaging has several limitations that make monitoring both responses to treatment and changes to healthy liver parenchyma after focal RT treatments challenging (26,27). Recent advances in imaging techniques, such as the use of gadoxetic acid–enhanced MRI as opposed to standard gadolinium-based MRI, have allowed for improvements in the diagnosis of liver tumors, the measurement of treatment responses, and the evaluation of liver function (28–34). This suggests that the use of this technique can inform clinical decision-making by providing further insights into both the efficacy and toxicity of treatment. First, this study demonstrated that the vast majority of patients (72% at 1–6 months and 65% at 6–12 months) experienced an FLR at follow-up MRI with median TDs of 35.4 Gy (median BED, 63.6 Gy) and 45.2 Gy (median BED, 88.7 Gy) at 1–6

Table 4: Adjusted Relative Risks from Multivariable Modified Poisson Regression Models to Identify Predictors of Liver Changes at 1–6 Months

Predictor	Multivariable Relative Risk [95% CI]	*P* Value
History of alcohol abuse		
No	Reference	
Yes	0.95 [0.73, 1.23]	.67
Hepatitis (B or C)		
No	Reference	
Yes	1.35 [1.00, 1.82]	.053
History of prior ^{90}Y		
No	Reference	
Yes	0.93 [0.72, 1.19]	.55
Baseline ALBI grade		
1	Reference	
2	0.77 [0.60, 0.99]	.04
3	0.61 [0.40, 0.91]	.01
Systemic therapy within 1 month		
No	Reference	
Yes	0.74 [0.57, 0.97]	.03
BED received, 30-unit increase	0.96 [0.80, 1.16]	.69

Note.—*n* = 91 scans. Scans evaluated by either rater are included. ALBI = albumin-bilirubin, ^{90}Y = yttrium 90.

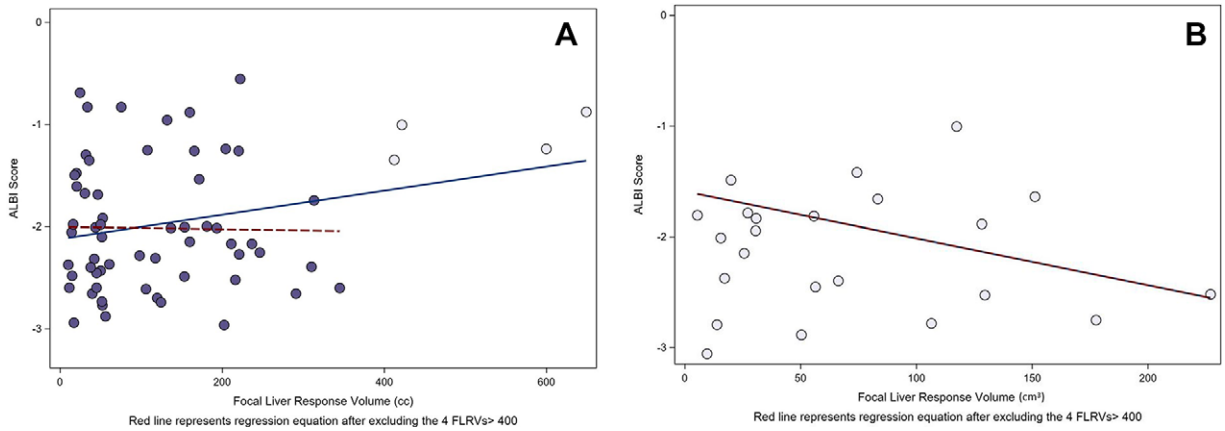


Figure 3: Associations between albumin-bilirubin (ALBI) score and focal liver response volume (FLRV) at the **(A)** 1–6-month time point and the **(B)** 6–12-month time point in patients with liver change. **(A)** Among the 63 patients with liver change at 6 months for whom ALBI and FLRV measurements were available, there was a significant linearly increasing association between FLRV and ALBI scores measured at 1–6 months ($P = .048$). For every 100-unit increase in the FLRV, the ALBI score increased by 0.12 units. **(B)** Among the 24 patients with liver change at 12 months for whom ALBI and FLRV measurements were available, there was no significant association between FLRV and ALBI scores measured at 6–12 months ($P = .37$).

months and 6–12 months, respectively. Second, we showed that FLR volume was related to changes in ALBI score at 1–6 months (P = .002) and that the ratio of FLR volume to total liver volume was associated with a worsening of ALBI scores at 1–6 months (P = .02). Finally, we reported histopathologic findings from explanted liver specimens.

Our study used gadoxetic acid–enhanced MRI to report the rate of FLRs at two time points in a large cohort of patients who were treated with a variety of RT fractionation regimens in the management of HCC, BTCs, and metastatic lesions. Our data demonstrated an FLR rate of 72% at 1–6 months and 65% at 6–12 months. These findings were similar to those of a CT-based series by Herfarth et al (4) that reported FLRs in 74% of patients at a median of 1.8 months after the completion of RT and a gadoxetic acid–enhanced MRI-based series by Sun et al (10) that reported FLRs in 80.1% of patients (38 of 47 patients). While Takeda et al (5) described peak changes at CT at 6 months and significant resolution at 9 months after the completion of RT, to our knowledge, our study is the first to report the rates of FLRs at two distinct time points using MRI. In addition, we found that approximately 15% of patients who developed FLRs demonstrated complete resolution 6–12 months after finishing RT. Additionally, no patients without FLRs at 1–6 months developed FLRs at a later time point. Given the lack of consensus guidelines regarding how to assess radiologic changes in irradiated liver parenchyma, our study may be particularly useful in informing further treatment decisions and toxicity management in patients who have undergone liver RT.

A number of TDs for FLRs have been described in the literature for both CT-based and MRI-based studies. CT-based studies have reported values ranging from 13.7 Gy in one fraction at 2 months to approximately 30 Gy in five fractions at 6 months, whereas MRI-based studies have reported values of 34.4 Gy over a median of 16 fractions at 1 month and 25–30 Gy in five fractions at 6 months (9,10). In our study, the median TD for FLRs was 35.4 Gy at 1–6 months and 45.2 Gy at 6–12 months, values that are slightly higher than those reported in prior series. To standardize these values and allow for a comparison across studies, we also calculated the BED (using an α/β ratio of 8 for normal liver parenchyma). In doing so, we found reported BED values associated with FLRs ranging from 37.2 Gy (13.7 Gy in one fraction) to 52.5 Gy (30 Gy in five fractions) (16). In comparison, the median threshold BED values for FLRs in this study were 63.6 Gy at 1–6 months and 88.7 Gy at 6–12 months.

Additionally, we aimed to determine if there were significant differences between the TDs, BEDs, and FLR volume measurements over time. One prior CT-based study demonstrated a peak incidence of FLRs at 6 months with significant resolution by 9 months (6), while another reported a 40% reduction in FLR volume at 2–4 months (4). Resolution of FLRs, however, has not been well-documented in studies in which MRI is performed for follow-up imaging, and no prior studies have reported the TDs and BEDs associated with these changes over time. Herein, we report a significant reduction in FLR volume and an increase in both the TD and BED associated with FLRs at 1–6 months as compared with 6–12 months. These findings may suggest varying degrees of healing of irradiated liver tissue and may also explain the higher TD and BED values in our study, because our data were collected at later time points than in prior studies. The focal RILD appears to be a reversible process, at least in regions of liver receiving lower doses of radiation.

Previous studies have attempted to correlate outcomes of FLRs with clinical factors, but their results have thus far been inconclusive. For example, Sanuki et al (9) reported lower TDs for FLRs in healthier livers (Child-Pugh class A compared with Child-Pugh class B), while the MRI-based study by Sun et al (10) found that patients demonstrating poorer liver function (with higher levels of total bile acid, total bilirubin, direct bilirubin, and α-fetoprotein) were less likely to demonstrate FLRs. To further evaluate this question, we used the ALBI score to measure liver function in the setting of FLR volume measurements. This method was used to minimize potential biases in retrospectively assessing for the degree of ascites and encephalopathy (both used in the Child-Pugh score) (17). Our data support the findings by Sun et al (10) that patients with poorer liver function (ALBI grades 2 and 3) are less likely to demonstrate FLRs compared with patients with better underlying liver function. This may be explained by poor hepatic parenchymal hepatobiliary phase contrast excretion in approximately half of patients who did not demonstrate an FLR, which may have obscured the accuracy of MRI readings (35). Additionally, it remains unclear how the receipt of systemic therapy may further influence these findings.

Furthermore, our study demonstrated that FLR volume at 1–6 months was associated with a significant increase in ALBI score at 1–6 months (P = .048), but not at 6–12 months. Similarly, the ratio of FLR volume to healthy liver volume was also positively associated with a significant increase in ALBI scores (P = .02). Both findings support the theory that development of FLRs is associated with some degree of transient liver toxicity. It remains unclear how this may affect clinical outcomes in patients. However, in our practice we exclude regions of FLR from our normal liver parenchyma contours in cases of reirradiation to ensure that an adequate volume of liver is spared from potential radiation toxicity, and we use FLR as additional assurance that our target lesion was accurately treated.

Although patients without FLRs in our study had no visible RT-related changes at MRI, they appeared more likely to experience significant worsening of liver function at 1–6 months. This suggests that although FLRs are associated with some degree of liver damage, patients without FLRs may have even worse baseline liver function and thus are significantly more sensitive to the effects of RT. Therefore, these patients may benefit from additional monitoring and/or interventions aimed at reducing the risk of further hepatic decompensation following RT. The lack of differences at 6–12 months may be related to some degree of toxicity resolution or may possibly be attributable to a reduced sample size and/or selection bias at the later time point.

Our study demonstrated no relationship between presence or volume of FLRs at 1–6 months and the OS at 1–6 months or 6–12 months. However, there was a trend toward reduction in OS associated with FLR volume at 6–12 months, which may signal that patients with impaired liver recovery after RT may be

at risk for worse outcomes. Additional data are necessary to corroborate these findings, however.

We also report the histopathologic findings for patients with FLRs at MRI who subsequently underwent liver transplantation. Our study demonstrated findings of RILD in all seven cases that were available for analysis, suggesting that the liver parenchymal changes observed at MRI may be associated with the development of RILD. The histopathologic findings in this analysis were similar to the CT-based FLR study by Olsen et al (12), who described three zones of parenchymal changes in the previously irradiated regions of the liver. Their report included a central area of necrotic tissue surrounded by a region of fibrosis, which was further encompassed by a zone of veno-occlusive disease. The specimens in this study exhibited very similar findings, with differing degrees of necrosis, fibrosis, and veno-occlusive disease present in each specimen. However, we also report case-specific differences that have not yet been previously detailed in the literature. Our findings offer insight into how the presence of FLRs may relate not only to the patterns of change described above, but also to additional factors such as tumor response and the cause of cirrhosis. While our pathologic findings represent an interesting correlate to the radiographic findings, more research is needed to improve our understanding of how these findings may alter gadoxetic acid metabolism during MRI and improve our overall interpretation of surveillance imaging after liver radiation.

This study had some limitations. Primarily, the retrospective nature of the study may prevent a full accounting of the clinical factors associated with FLRs owing to the biases and confounding variables that are inherent to such studies. Additionally, some patients who underwent RT did not undergo follow-up MRI after completing treatment. While this may have been related to factors such as insufficient insurance coverage or physician preference, it may also have been related to patient deterioration or death, which would have biased our results. Finally, each of the seven pathologic specimens that were available for analysis were from patients who demonstrated FLRs. It is unclear if these findings would be generalizable to patients who did not demonstrate FLRs.

To our knowledge, this is the largest and most comprehensive analysis of FLRs using MRI in patients who had undergone RT for tumors of the hepatobiliary system. We report the incidence of FLR after RT, the associated TD and/or BED values, and how these findings evolve over time. Better understanding of this phenomenon may allow for more accurate interpretation of surveillance imaging, and correlation with ALBI scores may be useful both as a predictor of FLR development and as a measure of liver toxicity following RT.

Author contributions: Guarantors of integrity of entire study, **A.D.N., M.B.**; study concepts/study design or data acquisition or data analysis/interpretation, all authors; manuscript drafting or manuscript revision for important intellectual content, all authors; approval of final version of submitted manuscript, all authors; agrees to ensure any questions related to the work are appropriately resolved, all authors; literature research, **A.D.N., K.K.S., T.W., F.K., B.T., M.B.**; clinical studies, **A.D.N., F.K., S.C.W., M.B.**; experimental studies, **A.D.N., T.W.**; statistical analysis, **A.D.N., E.M., M.B.**; and manuscript editing, **A.D.N., K.K.S., F.K., S.C.W., E.M., B.T., M.B.**

Disclosures of conflicts of interest: **A.D.N.** No relevant relationships. **K.K.S.** No relevant relationships. **T.W.** No relevant relationships. **F.K.** No relevant relationships. **C.K.K.** No relevant relationships. **S.C.W.** Grant payments paid to institution for salary support from Neuroendocrine Tumor Research Fund 2020 Pilot Award and Boehringer Ingelheim; consulting fees for research consensus panel from AstraZeneca; legal consultation payments to author from Heidell, Pittoni, Murphy & Bach and Martin Clearwater & Bell. **E.M.** Statistical support for this publication was supported in part by the NCI Cancer Center Support Grant P30CA196521-01 awarded to the Tisch Cancer Institute of the Icahn School of Medicine at Mount Sinai and used the Biostatistics Shared Resource Facility. **B.T.** No relevant relationships. **M.B.** No relevant relationships.

References

1. Lee P, Sioshansi S. Outcomes of SBRT for HCC in Patients with Child-Pugh B and C Cirrhosis. Int J Radiat Oncol Biol Phys 2018;102(3):S136.
2. Lischalk JW, Repka MC, Unger K. Radiation therapy for hepatobiliary malignancies. J Gastrointest Oncol 2017;8(2):279–292.
3. Mahadevan A, Blanck O, Lanciano R, et al. Stereotactic Body Radiotherapy (SBRT) for liver metastasis - clinical outcomes from the international multi-institutional RSSearch® Patient Registry. Radiat Oncol 2018;13(1):26.
4. Herfarth KK, Hof H, Bahner ML, et al. Assessment of focal liver reaction by multiphasic CT after stereotactic single-dose radiotherapy of liver tumors. Int J Radiat Oncol Biol Phys 2003;57(2):444–451.
5. Takeda A, Oku Y, Sanuki N, et al. Dose volume histogram analysis of focal liver reaction in follow-up multiphasic CT following stereotactic body radiotherapy for small hepatocellular carcinoma. Radiother Oncol 2012;104(3):374–378.
6. Sanuki-Fujimoto N, Takeda A, Ohashi T, et al. CT evaluations of focal liver reactions following stereotactic body radiotherapy for small hepatocellular carcinoma with cirrhosis: relationship between imaging appearance and baseline liver function. Br J Radiol 2010;83(996):1063–1071.
7. Shimizu A, Kobayashi A, Motoyama H, et al. Features of acute liver congestion on gadoxetate disodium-enhanced MRI in a rat model: Role of organic anion-transporting polypeptide 1A1. J Magn Reson Imaging 2015;42(3):828–836.
8. Hidaka M, Takatsuki M, Okudaira S, et al. The expression of transporter OATP2/OATP8 decreases in undetectable hepatocellular carcinoma by Gd-EOB-MRI in the explanted cirrhotic liver. Hepatol Int 2013;7(2):655–661.
9. Sanuki N, Takeda A, Oku Y, et al. Threshold doses for focal liver reaction after stereotactic ablative body radiation therapy for small hepatocellular carcinoma depend on liver function: evaluation on magnetic resonance imaging with Gd-EOB-DTPA. Int J Radiat Oncol Biol Phys 2014;88(2):306–311.
10. Sun XL, Jiang X, Kuang Y, et al. Potential of Gd-EOB-DTPA as an imaging biomarker for liver injury estimation after radiation therapy. Hepatobiliary Pancreat Dis Int 2019;18(4):354–359.
11. Michel R, Françoise I, Laure P, Anouchka M, Guillaume P, Sylvain K. Dose to organ at risk and dose prescription in liver SBRT. Rep Pract Oncol Radiother 2017;22(2):96–102.
12. Olsen CC, Welsh J, Kavanagh BD, et al. Microscopic and macroscopic tumor and parenchymal effects of liver stereotactic body radiotherapy. Int J Radiat Oncol Biol Phys 2009;73(5):1414–1424.
13. Murray LJ, Sykes J, Brierley J, et al. Baseline Albumin-Bilirubin (ALBI) Score in Western Patients With Hepatocellular Carcinoma Treated With Stereotactic Body Radiation Therapy (SBRT). Int J Radiat Oncol Biol Phys 2018;101(4):900–909.
14. Gui B, Weiner AA, Nosher J, et al. Assessment of the Albumin-Bilirubin (ALBI) Grade as a Prognostic Indicator for Hepatocellular Carcinoma Patients Treated With Radioembolization. Am J Clin Oncol 2018;41(9):861–866.
15. Koay EJ, Owen D, Das P. Radiation-Induced Liver Disease and Modern Radiotherapy. Semin Radiat Oncol 2018;28(4):321–331.
16. Son SH, Jang HS, Lee H, et al. Determination of the α/β ratio for the normal liver on the basis of radiation-induced hepatic toxicities in patients with hepatocellular carcinoma. Radiat Oncol 2013;8(1):61.
17. Su TS, Yang HM, Zhou Y, et al. Albumin - bilirubin (ALBI) versus Child-Turcotte-Pugh (CTP) in prognosis of HCC after stereotactic body radiation therapy. Radiat Oncol 2019;14(1):50.
18. Maturen KE, Feng MU, Wasnik AP, et al. Imaging effects of radiation therapy in the abdomen and pelvis: evaluating "innocent bystander" tissues. RadioGraphics 2013;33(2):599–619.
19. Koo TK, Li MY. A Guideline of Selecting and Reporting Intraclass Correlation Coefficients for Reliability Research. J Chiropr Med 2016;15(2):155–163.
20. Lujan ME, Brooks ED, Kepley AL, Chizen DR, Pierson RA, Peppin AK. Grid analysis improves reliability in follicle counts made by ultrasonography in women with polycystic ovary syndrome. Ultrasound Med Biol 2010;36(5):712–718.
21. Zou G. A modified poisson regression approach to prospective studies with binary data. Am J Epidemiol 2004;159(7):702–706.
22. Petersen MR, Deddens JA. A comparison of two methods for estimating prevalence ratios. BMC Med Res Methodol 2008;8(1):9.

23. Carter RE, Lipsitz SR, Tilley BC. Quasi-likelihood estimation for relative risk regression models. Biostatistics 2005;6(1):39–44.
24. Yelland LN, Salter AB, Ryan P. Performance of the modified Poisson regression approach for estimating relative risks from clustered prospective data. Am J Epidemiol 2011;174(8):984–992.
25. Tamhane AR, Westfall AO, Burkholder GA, Cutter GR. Prevalence odds ratio versus prevalence ratio: choice comes with consequences. Stat Med 2016;35(30):5730–5735. [Published correction appears in Stat Med 2017;36(23):3760.]
26. Kellock T, Liang T, Harris A, et al. Stereotactic body radiation therapy (SBRT) for hepatocellular carcinoma: imaging evaluation post treatment. Br J Radiol 2018;91(1085):20170118.
27. Geisel D, Lüdemann L, Hamm B, Denecke T. Imaging-Based Liver Function Tests--Past, Present and Future. Rofo 2015;187(10):863–871.
28. Ichikawa T, Sano K, Morisaka H. Diagnosis of Pathologically Early HCC with EOB-MRI: Experiences and Current Consensus. Liver Cancer 2014;3(2):97–107.
29. Kim SW, Joo I, Kim HC, et al. LI-RADS treatment response categorization on gadoxetic acid-enhanced MRI: diagnostic performance compared to mRECIST and added value of ancillary features. Eur Radiol 2020;30(5):2861–2870.
30. Campos JT, Sirlin CB, Choi JY. Focal hepatic lesions in Gd-EOB-DTPA enhanced MRI: the atlas. Insights Imaging 2012;3(5):451–474.
31. Kubota K, Tamura T, Aoyama N, et al. Correlation of liver parenchymal gadolinium-ethoxybenzyl diethylenetriaminepentaacetic acid enhancement and liver function in humans with hepatocellular carcinoma. Oncol Lett 2012;3(5):990–994.
32. Kamimura K, Fukukura Y, Yoneyama T, et al. Quantitative evaluation of liver function with T1 relaxation time index on Gd-EOB-DTPA-enhanced MRI: comparison with signal intensity-based indices. J Magn Reson Imaging 2014;40(4):884–889.
33. Esterson YB, Flusberg M, Oh S, Mazzariol F, Rozenblit AM, Chernyak V. Improved parenchymal liver enhancement with extended delay on Gd-EOB-DTPA-enhanced MRI in patients with parenchymal liver disease: associated clinical and imaging factors. Clin Radiol 2015;70(7):723–729.
34. Faletti R, Cassinis MC, Fonio P, et al. Multiparametric Gd-EOB-DTPA magnetic resonance in diagnosis of HCC: dynamic study, hepatobiliary phase, and diffusion-weighted imaging compared to histology after orthotopic liver transplantation. Abdom Imaging 2015;40(1):46–55.
35. Goodwin MD, Dobson JE, Sirlin CB, Lim BG, Stella DL. Diagnostic challenges and pitfalls in MR imaging with hepatocyte-specific contrast agents. RadioGraphics 2011;31(6):1547–1568.